Studies of positron scattering near excitation thresholds

Alexis Read

Thesis submitted for the degree of Master of Philosophy of the University of London. 2003

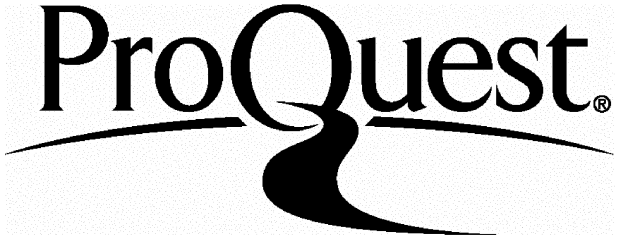

Abstract

Theoretical investigations have been made of positron scattering by a model one-electron atom whose lowest excitation threshold energy lies below the threshold for positronium formation. The principle purpose of this work has been to find out if there is any enhancement in the positron-electron annihilation rate near to the excitation threshold, as is known to exist near to the positronium formation threshold.

A model one-electron atom with the required properties was constructed, and this target system was then incorporated into the positron-atom scattering formalism. The Kohn variational method was then used to calculate the elastic scattering phase shift and the associated total wave function at various energies in the range from zero up to the lowest excitation threshold of the model atom. The energy dependence of the positron-electron annihilation rate was then determined from the total wave function at the positron-electron coalescent point. A significant enhancement of the annihilation rate was observed close to the excitation threshold, suggesting that there may well be similar enhancement at other inelastic thresholds and resonances below the positronium formation threshold.

The elastic scattering wave function has also been used to determine the angular correlation of the annihilation radiation, which provides information about the momentum distribution of the positron-electron pair at the moment of annihilation.

Acknowledgements

I would like to extend my thanks to my supervisor, Prof. J. Humberston, for his patient support, lucid explanations, extensive knowledge in the field of positron physics, and his more general help in my work for this thesis. He has been invaluable in his encouragement and for my personal advancement in scattering theory and other aspects of physics.

I would also like to thank Dr P. Van Reeth and Dr J. Dunn for their support in data analysis, and in the experience in computer modelling that they have extended to me.

Additional thanks for their support go to Dr R. Bannocks, the Group C research body and the whole of the Department of Physics and Astronomy at UCL.

Finally I would like to express my gratitude for the financial assistance of the Engineering and Physical Sciences Research Council for the research grant, and the Department of Physics and Astronomy at UCL for financial support for attending national conferences.

Contents

Abstract 1

Acknowledgements 1

1 Introduction 3
- 1.1 Properties of the positron 5
- 1.2 Positronium 7
- 1.3 Current work with positrons 8

2 The Model Atom 12
- 2.1 The Rayleigh-Ritz method 13
- 2.2 Integration techniques 19

3 The Kohn Variational Method 20
- 3.1 The trial scattering wave function 20
- 3.2 The Kohn functional 22
- 3.3 The total wave function and short range terms 24
- 3.4 Schwartz Singularities 27

4 Positron-model atom Scattering 28
- 4.1 The stabilisation technique 32
- 4.2 Virtual excitation 33

5 Annihilation in Positron-atom Scattering 39
- 5.1 Annihilation Rate 39
- 5.2 Angular Correlation 41

6 Summary and Conclusions 45

Bibliography 46

Chapter 1

Introduction

The theory of collisions plays a central role in many branches of physics, achieving considerable success in clarifying our understanding of a wide variety of processes in molecular, atomic and subatomic physics. The study of positron scattering is valuable as a testbed for collision theory as it is sufficiently distinct from well-known systems featuring electron interactions.

As a consequence of Dirac's paper on the relativistic theory of the electron [Dir28], the existence of the positron was first postulated. This can be considered as one of the main theoretical achievements of 20th century physics, and a validation of both the quantum theory of matter and the theory of special relativity which preceded it by 20 years.

Dirac's postulate was based on the Schrödinger equation,

$$i\hbar\frac{\partial}{\partial t}\Psi = H\Psi, \tag{1.1}$$

where H is the total Hamiltonian. In a relativistic theory the spatial coordinates must be on the same footing as the time coordinate i.e. points in space-time are defined by $(x_1, x_2, x_3, x_4 = ict)$. Dirac proposed a wave equation derived from the Schrödinger equation that would hold for relativistic

velocities i.e. the Hamiltonian has a linear momentum and mass component.

$$i\hbar\frac{\partial}{\partial t}\Psi = -i\hbar c\sum_{k=1}^{3}\alpha_k\frac{\partial}{\partial x_k}\Psi + \beta m_0 c^2\Psi, \tag{1.2}$$

where m_0 is the rest mass of the electron and α and β are constants expressed by 4×4 matrices. The wave function Ψ thus needs to have four components, the first two corresponding to the 1/2 spin states of the electron, and the second two to a negative energy equivalent. The total energy E for a free electron conforming to this equation is then given by:

$$E^2 = p^2c^2 + m_0^2c^4, \tag{1.3}$$

where p is the momentum of the particle, m_0 is the rest mass and c is the speed of light in a vacuum. The positive root corresponds to the energy of a normal electron, and the negative root, between $-m_0c^2$ and -∞, corresponds to an electron in a negative energy level.

There are several ways to look at the physical representation of the positron. Dirac first proposed that space be composed of a sea of negative energy electrons with all the negative energy states occupied, so that, due to the Pauli exclusion principle, there are no available states for real electrons to fall into. Excitation of one of these negative energy electrons (by a photon) by $\Delta E > 2m_0c^2$ creates a real electron with a positive energy, leaving a hole in the sea of negative energy states. This hole has the properties of the positron, i.e. the same mass as the electron but opposite sign of the charge.

The existence of the positron, and the possibility of electron-positron pair production were confirmed experimentally by Anderson in 1932. However, to fully explain the existance of antiparticles, quantum field theory (introduced by R. P. Feynman, J. Schwinger and S. Tomonaga) must be used. Subsequent representations of the positron have had to accomodate the existance all other antiparticles, for example, Feynman's representation involves reversing the direction of the particle through time to achieve the antiparticle state.

1.1 Properties of the positron

The positron has the same spin, mass and magnitude of charge (but opposite sign) as the electron. As a consequence of CPT symmetry - charge conjugation (C), parity exchange (P) and time reversal (T), the positron also has the same gyromagnetic ratio as the electron.

After the discovery of the positron, the fundamental properties of positrons were investigated to verify the theoretical predictions. As with the electron, there are several components to the interaction between the positron and an atomic target for low energy collisions that concern us here. The static component arises from the interation between the projectile and the undistorted target, and it affects both the electron and the positron at all energies. Conversely, the polarisation interaction is effective only at low energies such that the electron cloud around the target has time to be polarised by the projectile. The exchange interaction affects only electrons and is most effective when the projectile and the target electrons have similar kinetic energies [KS90].

Interaction/ Collision Process	Incident Particle	
	positron	electron
Static	repulsive	attractive
Polarisation	attractive	attractive
Exchange	no	yes
Positronium Formation	yes	no
Annihilation	yes	no

Table 1.1: A summary of the differences and similarities between the interactions and processes involved in electron-atom and positron-atom scattering.

At high collision energies the total cross-sections for positron-atom and electron-atom scattering merge, as the static interaction begins to dominate. At lower energies, as shown in figure 1.1, the total cross-section for positron scattering tends to be smaller than that for electron scattering due to the partial cancellation of the static and polarisation terms in the interaction potential.

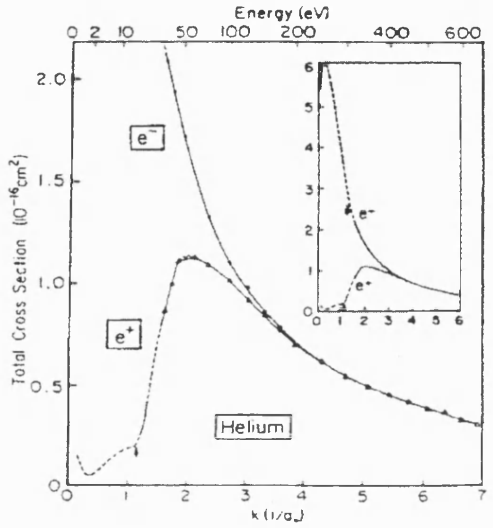

Figure 1.1: The total cross sections for positron and electron scattering by helium. [KSS+81], 0-600eV

Positrons are produced in two main ways; through pair production by sufficiently high energy photons, or by the radioactive β^+-decay of certain radioisotopes. The most common isotope used in experiments is ^{22}Na, as its branching ratio for β^+ -decay is 91% and the half life is 2.6 years [CH01]. This allows an acceptable beam intensity with a much reduced preparation time. The energies of the ejected positrons, also known as β^+ particles, are approximately 0.5 eV after moderation in a material such as tungsten.

One unique process that antimatter can undergo is annihilation of electrons and positrons, producing either two or three high energy γ-rays. The fastest process is production of two γ-rays, each having an energy of 511 keV, from annihilation of the singlet state of the electron-positron pair. Three γ-rays are produced from a triplet state pair, with a total energy of 1022 keV. The angular distribution of the two γ-rays in the annihilation in the singlet state can reveal information about the momentum distribution of the positron-electron pair just before annihilation.

1.2 Positronium

The bound state of a positron and an electron is called positronium (Ps), and represents the second process specific to positron collisions. This was first predicted by Mohorovičić in 1934, and expanded upon by Ruark [Rua45].

Positronium, with a reduced mass of half the electron mass, has energy levels half those of the hydrogen atom, excepting the hyperfine separations of the energy levels. This is due firstly to the large magnetic moment of the positron as compared to the proton, and secondly to QED effects within the atom. The ground state energy of positronium is 6.8 eV. Positronium exists in two total spin states, S = 0 (singlet state) where the spins of the positron and electron are antiparallel, known as para-positronium, and S = 1 (triplet state) where the spins are parallel, known as ortho-positronium. The ratio of creation of these states is 3:1, ortho-Ps to para-Ps. The S = 1 state must decay to an odd number of γ-rays (three) due to spin and parity conservation, with the singlet state producing two γ-rays. The lifetimes of these states is 142 ns for ortho-Ps but only 125 ps for the para form [CH01]. This, in addition to the creation ratio, gives an overall annihilation rate ratio of 1:370, ortho-Ps to para-Ps. Positronium itself can bind to some atomic systems, eg. electron-positronium, Ps^- (predicted by Wheeler [Whe46], discovered by Mills [Mil81]), molecular positronium Ps_2 and positronium hydride PsH [RM97]. Furthermore, strong evidence has been published of positron and positronium binding to other atoms [RMV98].

The threshold energy for positronium formation in positron collisions with an atom is $E_{Th} = E_I - E_{Ps}$, where E_I is the ionisation energy of the target atom and E_{Ps}= 6.8 eV is the binding energy of positronium. The next threshold is usually the first excitation state of the target atom, E_{ex}. It is not necessarily the lowest threshold as that for electron induced excitation because positrons cannot change the target electrons' spin during a collision. For some atoms, such as the alkalis, the outer electron is so weakly bound that positronium can be formed even when the incident positron energy is zero, i.e. $E_I \leq E_{Ps}$. Positronium formation is then exothermic - the positronium emerges from the collision with more kinetic energy than that of the incoming positron. For most other atoms, positronium formation is an endothermic process, where $E_I \geq E_{Ps}$. The energy region between E_{Th} and E_{Ex} is known as the Ore gap [Ore49], within which only two scattering processes can occur, namely:

$$e^+ + He \rightarrow \quad e^+ + He \quad \text{(elastic scattering)} \tag{1.4}$$
$$\rightarrow \quad Ps + He^+ \quad \text{(positronium formation).} \tag{1.5}$$

In adddition, electron-positron annihilation is always possible, although it has a very low cross section.

In this study, we will only look at energies around this region, as modelling the scattering at higher energies increases the number of reaction channels available, with an accompanying increase in calculation and complexity.

1.3 Current work with positrons

Since the discovery of positrons, much research has been undertaken using them. Initial work focussed on discovering their properties, but with the advent of monoenergetic positron beams in the early 1970s, and advances in computing, it has been possible to obtain scattering cross-sections for individual collision processes and verify them theoretically with *ab initio* calculations for simple target systems.

Now that the properties of positrons are well known, they have been useful as probes for other experiments such as understanding gamma-ray spectra of astrophysical origin [RL94], positron binding to atoms [RM97], positron-induced ionization and fragmentation of molecules [HDX+93], and the characterisation of thin films, materials, and material surfaces [SL88]. Positrons are also used in *positron emission tomography* (PET) to map out areas of the brain.

Experiments at CERN in Geneva [BBB+96] and Fermilab near Chicago [BCG+98] created the first antihydrogen atoms by passing very high energy (~1.2 GeV) antiprotons through a target. More recently very low energy antihydrogen atoms have been created at CERN by an experimental collaboration called ATHENA. Here the antihydrogen was produced by mixing trapped antiprotons and positrons in a cryogenic environment. Cooling of the mixed particles was done by synchrotron radiation inside a Penning trap, to yield the antihydrogen [AAB+]. Additionally, a second team called ATRAP

at CERN has observed antihydrogen via a different method of separating the antihydrogen atom into its constituent positron and antiproton particles, and trapping the antiprotons to verify this dissociation. The magnitude of the electric field required to separate the antihydrogen is measured, and provides the first glimpse into the structure of antihydrogen [?].

Antihydrogen atoms allow an important test of CPT symmetry to be made, as tests on them are potentially the most accurate method; comparisons of the 1s-2s spectra of antihydrogen and hydrogen should find them identical. The availability of antihydrogen will enable tests on the interaction of antimatter with gravity - a test of the weak equivalence principle (WEP).

Recently, Surko and Gribakin [IGG+00] have been working on both the theory and experiment of positron annihilation on molecules. Their framework describes two main mechanisms for annihilation, direct and resonant annihilation, and the theoretical prediction compares favourably with the experimental results. This annihilation is highly sensitive to changes in the molecular structure, with up to five orders of magnitude difference between the annihilation rates $(10^3 - 10^8)s^{-1}$ for different molecules. This sensitivity is mainly attributed to the resonant annihilation mechanism. Their paper [IGG+00] entails the first study of positron annihilation as a function of positron energy, and the results provide direct evidence that resonances of the positron-molecule complex associated with vibrational excitation of the molecule are responsible for the greatly enhanced annihilation rates in some molecules. They additionally provide results, demonstrating that positrons bind to molecules. Rather than study vibrational excitation in molecules, we have chosen to study electronic excitation of a simple atom.

Positron annihilation rates for atoms and molecules are often expressed in terms of:

$$Z_{eff} = \Gamma/(r_0^2 c n_m), \tag{1.6}$$

where Z_{eff} is the effective number of electrons in the target system, Γ is the measured annihilation rate, r_0 is the classical radius of the electron, and n_m is the molecular number density. As the low energy positron distorts the target atom on its approach, Z_{eff} is usually not equal to the actual number of electrons in the target atom. The value of Z_{eff} is thus dependent upon

the incident speed of the positron. For butane Z_{eff} was measured at around 10^4, a huge enhancement over Z, the number of electrons in the molecule. There have been several proposals to explain this in terms of an electronic or vibrational resonance, or a positron-molecule bound state [SPLW88, IGG$^+$00, LW97, dGL96]. The presence of either a resonance or a bound state would most likely result in a long-lived positron-molecule complex, thus increasing the probability of annihilation.

A model of this phenomenon was developed by Gribakin [Gri00] which considers two mechanisms. Where $Z_{eff} \leq 10^3$, such as for small molecules, the enhancement is explained in terms of *virtual* bound states involving correlations between the positron and the molecular electrons. For $Z_{eff} \geq 10^3$, the mechanism involves positron capture in vibrational *Feshbach* resonances, that is, resonances involving the motion of the atomic nuclei. An incident low-energy positron might then excite a vibrational mode of the positron-molecule complex and become temporarily bound to the molecule, increasing the probability of annihilation. This model scales well with molecular size; the number of vibrational resonances increases in proportion to the rapid increase in Z_{eff} which has been experimentally measured.

This thesis follows on from the work done by J.T. Dunn [Dun02] on resonances in positron-helium scattering, where *ab initio* calculations using accurate model potentials [Pea82] revealed a resonance-type structure in the s-wave elastic scattering cross section at an energy just below E_{Ps}, the threshold energy for positronium formation. This feature is attributed to the model atom as experiments have not found this resonance in real positron-helium collisions. Nevertheless, it does verify the model made by Gribakin in that the positron remains trapped around the helium atom for much longer than the usual collision time, in a resonant state with the model atom. Correspondingly, this shows a large increase in Z_{eff} similar to that predicted by Gribakin's model.

The existance of the virtual state is best described as capture of an electron by the positron, although the resulting positronium is then bound to the residual ion and cannot escape. Instead, dissociation of the positronium takes place into a free positron with the electron recaptured by the ion, resulting in an enhanced positron-helium interaction time, and therefore an enhanced annihilation rate.

Substantial enhancement of the annihilation rate has also been calculated

close to the Ps formation threshold [VH98a], and therefore it is interesting to investigate if there is enhancement of annihilation at any inelastic threshold. This thesis looks at just that: to investigate whether there is such an enhancement at the excitation threshold for an atom. The ehancement would indicate the degree of correlation between the positron and the atom. These results in turn can be used as a guide when examining annihilation at excitation thresholds in more complex experimental environments such as molecules. No atom has its lowest excitation threhold below the positronium formation threshold, so it is neccessary to create a model atom with this property if we intend to model annihilation at this threshold because, in our time-independent formalism, the annihilation rate at energies beyond the positronium formation threshold is infinite [VH98b].

Chapter 2

The Model Atom

The extension of Dunn's work involves attempting to use similar scattering methods for an artificial atom. To limit the complexity of such an arrangement, a decision was taken to use a one-electron atom model with a modified Coulomb potential between the electron and the 'nucleus'.

The modified electron-nucleus potential is taken to have the form:

$$V^- = V_e(r_2) = -\frac{1}{r_2} - Ae^{-Br_2}. \tag{2.1}$$

The exponential term in the above potential is included to enhance the attractive force, and thereby increase the binding energy of the atom, so that the energy of the first excited state is below the threshold for positronium formation. The Rayleigh-Ritz variational method is used to calculate the binding energy of the electron in the potential V^- for a specific choice of values of A and B. The values of these parameters are then changed until the required binding energy is obtained. The graph showing the potential $V^-(r_2)$ is given in figure (2.2):

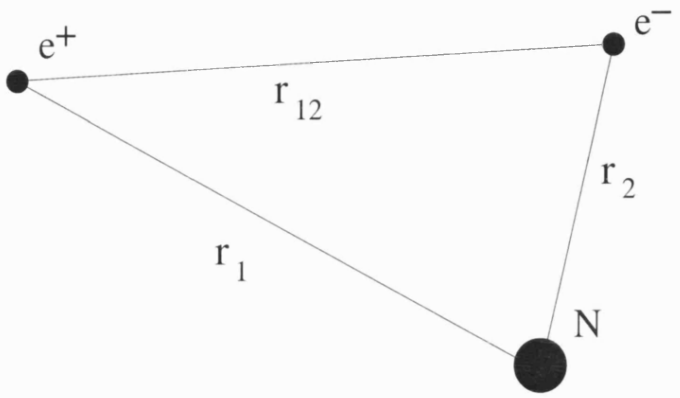

Figure 2.1: The positron-atom coordinate system.

The normal Coulomb potential function for the hydrogen atom is given for comparison.

2.1 The Rayleigh-Ritz method

Due to the form of the model potential function, it is not possible to obtain exact results for the binding energy, and an approximation method must be used. The Rayleigh-Ritz method is commonly used to find solutions to bound state problems. The functional in equation (2.2) yields the exact energy E_n, for the Hamiltonian H, when $\Phi_n^t|H$, the trial wave function equals the exact wave function ϕ_n:

$$I = < \Phi_n^t|H - E_n|\Phi_n^t > \tag{2.2}$$

The Rayleigh-Ritz method makes use of stationary properties arrived at by

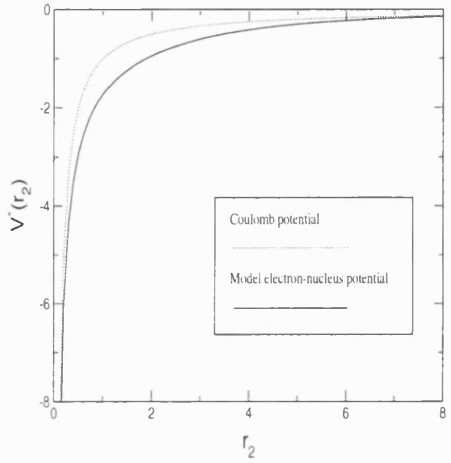

Figure 2.2: The model electron-nucleus potential function $V^-(r_2) = -\frac{1}{r_2} - Ae^{-Br_2}$ and the pure Coulomb function $V^-(r_2) = -\frac{1}{r_2}$.

considering how the value of the functional changes with respect to variations in Φ_n^t away from the exact solution of the Schrödinger equation, ϕ_n. i.e. $\delta I = 0$ states that the functional I, which is a function of a function of the system considered, is stationary with respect to small variations. Associated with the eigenvalues E_n are an orthonormal set of eigenfunctions ϕ_n, i.e. $H\phi_n = E_n\phi_n$. If the function ϕ is not known exactly, then we use a trial function which depends on a finite set of variational parameters $(\alpha_1, \alpha_2, ..., \alpha_n)$, and Φ_n^t will give E_n if:

$$\frac{\partial I}{\partial \alpha_i} = 0 \qquad i = 1, 2, \ldots, n, \tag{2.3}$$

which leads to a set of n linear simultaneous equations which can be solved to determine the eigenvalues and the associated eigenvectors. Φ_n^t differs from the exact eigenfunction ϕ_n by $\delta\phi$ so:

$$\Phi_n^t = \phi_n + \delta\phi. \tag{2.4}$$

Therefore, substituting into the functional and using the hermiticity of H, we can rewrite I as:

$$\begin{aligned} I &= <\phi_n + \delta\phi|H - E_n|\phi_n + \delta\phi> & (2.5)\\ &= <\phi_n|H - E_n|\phi_n> + 2<\delta\phi|H - E_n|\phi_n> \\ &\quad + <\delta\phi|H - E_n|\delta\phi>. & (2.6) \end{aligned}$$

The first two terms on the right hand side are zero as $(H - E_n)|\phi_n> = 0$, so equating (2.2) and (2.6) we can obtain:

$$<\Phi_n^t|H - E_n|\Phi_n^t> \equiv <\delta\phi|H - E_n|\delta\phi> = \delta I = 0. \tag{2.7}$$

The stationary property is preserved as $<\delta\phi|H - E_n|\delta\phi>$ and $<\delta\phi|\delta\phi>$ are of second order in $\delta\phi$, so can be discarded if we take equation (2.7) to first order in $\delta\phi$. This leaves us with the Rayleigh-Ritz functional:

$$E_n^v = \frac{<\Phi_n^t|H|\Phi_n^t>}{<\Phi_n^t|\Phi_n^t>}. \tag{2.8}$$

This functional provides a variational estimate of the energy of the system which is a rigorous upper bound on the lowest eigenvalue, E_1, of H, that is $E_n^v \geq E_1$. E_n^v has a second order dependence on $\delta\phi$ and so has the required stationary property. The proof that the variational estimate of the energy is an upper bound arises from the expansion of Φ_n^t in terms of the complete set of orthonormal eigenfunctions of H:

$$\Phi_n^t = \sum_j c_j\phi_j, \tag{2.9}$$

so the Rayleigh-Ritz functional has the form:

$$E_n^v = \frac{<\sum_i c_i\phi_i|H|\sum_j c_j\phi_j>}{<\sum_i c_i\phi_i|\sum_j c_j\phi_j>} \tag{2.10}$$

$$= \frac{\sum_{i,j} E_j c_j c_i <\phi_i|\phi_j>}{\sum_{i,j} c_j c_i <\phi_i|\phi_j>} \tag{2.11}$$

which, as ϕ_i form an orthonormal set, i.e. $<\phi_i|\phi_j> = \delta_{ij}$, reduces to:

$$E_n^v = \frac{\sum_j |c_j|^2 E_j}{\sum_j |c_j|^2}. \tag{2.12}$$

Subtracting E_1 from both sides gives:

$$E_n^v - E_1 = \frac{\sum_j |c_j|^2 (E_j - E_1)}{\sum_j |c_j|^2}. \tag{2.13}$$

Now $E_j \geq E_1$ for all j, so $E_n^v \geq E_1$. The trial function is inserted into the Rayleigh-Ritz functional, and the set of of n-simultaneous equations solved to give the parameter values c_i $(i = 1, \ldots, n)$ for the lowest value of the functional, and the coresponding eigenvalue.

These n-simultaneous linear homogeneous equations can be expressed as the matrix eigenvalue equation:

$$(\mathbf{H} - E_n^v \mathbf{A})\boldsymbol{\alpha} = 0, \tag{2.14}$$

where $\boldsymbol{\alpha}$ is a column matrix listing the optimum values of the linear coefficients c_i in the variational wave function, and:

$$H_{ij} = <\phi_i|H|\phi_j>, \tag{2.15}$$

$$A_{ij} = <\phi_i|\phi_j>. \tag{2.16}$$

The eigenvalues $E_1^v, E_2^v, E_3^v, \ldots$ can also be obtained in addition to the optimised variational parameters. Increasing the number of terms in the basis

set allows a closer fit to the exact eigenvalues and eigenfunctions required, and a study of the rate of convergence of the eigenvalues with respect to the increasing number of parameters can then provide information on the accuracy of the results.

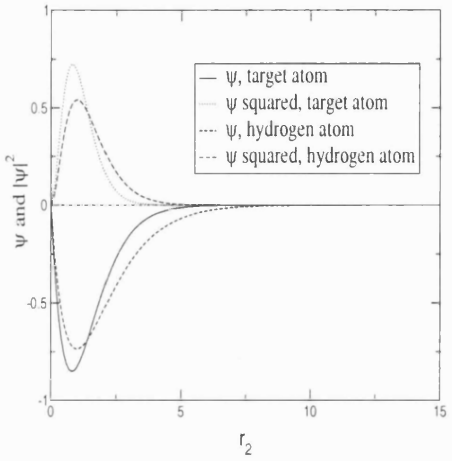

Figure 2.3: The electron wave function, and the square of its modulus, for the model atom and for the hydrogen atom. Ψ is given by $\Psi = r_2\Phi_T^t$ in the main text.

The form of the target wave function Φ_T^t is taken to be:

$$\Phi_T^t = e^{-\delta r_2} \sum_{k=1}^{N} \alpha_k r_2^{k-1} \tag{2.17}$$

The potential well is more attractive than the pure Coulomb form for all values of r_2 and therefore the model atom wave function is pulled in closer to the origin than is the hydrogen atom wave function, as can be seen in figure (2.3).

For the scattering process under investigation, we limit the number of reaction channels to two, elastic scattering and excitation. The second energy eigenvalue of equation (2.14), E_2, is an upper bound on the energy of the first excited state of the model atom. We require a model atom for which the energy of its first excited state, E_2, is $\leq$ -6.8 eV, so that the lowest excitation threshold is below the positronium formation threshold.

Using the Rayleigh-Ritz method with the trial wave function given by (2.17) and the potential given by (2.1), we have found the ground state and first excited state energies of the model atom, with the requirement that $E_2 \leq$ -6.8 eV, with the following parameters given in table (2.1).

Parameter	Value
E_1	-1.1687602 a.u.
E_2	-0.32147654 a.u.
δ	1.0
A	1.2
B	0.4
Polarizability	1.1697695

Table 2.1: The values of the potential parameters and the corresponding two lowest energy eigenvalues, and the dipole polarizability.

Convergence of the values of E_1 and E_2 with respect to the number of terms in the trial wave function Φ_T^L is displayed in figure (2.4).

As can be seen from the values of E_2 being less than -0.25 a.u. given in table (2.1), the model potential posesses the required features. The deeper potential well binds the electron tighter to the nucleus in both the ground state and the first excited state.

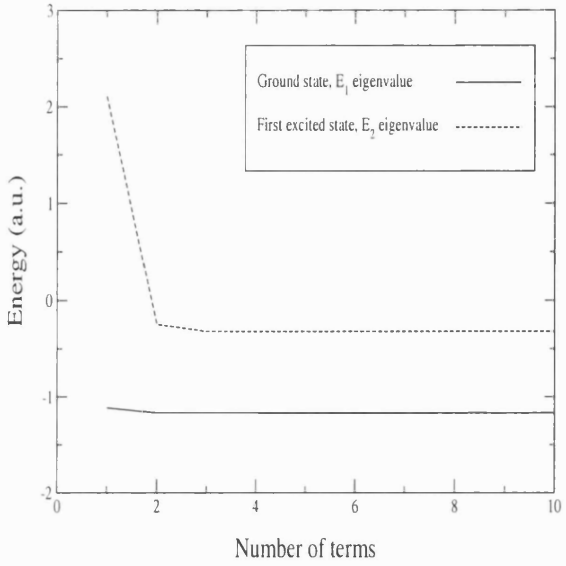

Figure 2.4: Convergence of the two lowest energy eigenvalues for the model potential with respect to increasing the number of terms in the trial wave function.

2.2 Integration techniques

The matrix elements in equation (2.15) and (2.16) are calculated using the *Gauss-Laguerre* numerical integration technique.

$$\int_0^\infty \exp^{-\alpha x} F(x)dx \approx \frac{1}{\alpha}\sum_{i=1}^{M} w_i F\left(\frac{x_i}{\alpha}\right), \tag{2.18}$$

where w_i are weights and x_i are abcissae dependent on i and M. The procedure is exact if F(x) is a polynomial of degree less than or equal to (2M - 1).

Chapter 3

The Kohn Variational Method

Rigorous bounded variational methods do exist for scattering theory; however it is more practical to sacrifice this rigorous bound for the sake of much less complexity in the Kohn variational method (Kohn 1948). Additionally, the Kohn method provides lower bounds on the diagonal elements of the K-matrix, under certain well-known circumstances, and can produce results with a very high accuracy for a good choice of the trial wave function.

3.1 The trial scattering wave function

In contrast to the bound state calculations using the Rayleigh-Ritz method, the trial wave functions used for the Kohn method are not normalisable. However, the scattering wave function can be derived by considering the asymptotic behaviour of a monoenergetic beam of particles; a plane wave with wavenumber k, elastically scattered by a central potential, V. The time-independent Schrödinger equation for the system is:

$$(-\nabla^2 + 2V(r))\psi_{sc}(\mathbf{r}) = k^2\psi_{sc}(\mathbf{r}). \tag{3.1}$$

In fact, the whole system is axially symmetric as the positron beam is planar, so the total wave function can be expanded in terms of the complete orthonormal set of Legendre polynomials, i.e.

$$\psi_{sc}(\mathbf{r}) = \sum_{l=0}^{\infty} B_l R_l(k,r) P_l(\cos\theta), \tag{3.2}$$

where B_l is a constant. The Laplacian operator in equation (3.1), ∇^2, is given in spherical polar coordinates by:

$$\nabla^2 = \frac{1}{r^2}\frac{\partial}{\partial r}(r^2\frac{\partial}{\partial r}) + \frac{1}{r^2\sin\theta}\frac{\partial}{\partial\theta}(\sin\theta\frac{\partial}{\partial\theta}) + \frac{1}{r^2\sin^2\theta}\frac{\partial^2}{\partial\phi^2} \tag{3.3}$$

and, taking L_{op} as the total angular momentum operator, we can reduce the second and third terms in the above operator to be simply $-L^2_{op}/r^2$. Since the Legendre polnomials $P_l(cos\theta)$ are eigenfunctions of L^2_{op} with eigenvalues $l(l+1)$, equation (3.3) can be reduced to a radial equation:

$$\left(-\frac{1}{r^2}\frac{d}{dr}(r^2\frac{d}{dr}) + \frac{l(l+1)}{r^2} + 2V(r)\right) R_l(k,r) = k^2 R_l(k,r), \tag{3.4}$$

and making the substitution $u_l(kr) = rR_l(k,r)$, this equation is further reduced to:

$$\left(-\frac{d^2}{dr^2} + \frac{l(l+1)}{r^2} + 2V(r)\right) u_l(kr) = k^2 u_l(kr). \tag{3.5}$$

The boundary conditions for this equation determine the solutions to this equation. As $R_l(k,r)$ must be finite everywhere, $u_l(kr_1) \to 0$ as $r \to 0$ and the asymptotic solutions beyond the range of the potential are:

$$u_l(kr) = N_l(k)r[j_l(kr) - \tan\eta_l n_l(kr)], \tag{3.6}$$

where $j_l(kr)$ and $n_l(kr)$ are the spherical Bessel and Neumann functions respectively, and η_l is the phase shift for the lth partial wave. V(r) must tend to zero faster than 1/r as $r \to \infty$ for this particular solution.

The form of the trial wave function ψ_{sc} to be used in the Kohn method is merely an approximation of $u_l(kr)/r$, and thus has the same form and boundary conditions:

$$\psi_{sc}(kr) \underset{r\to 0}{\sim} r^l \tag{3.7}$$

$$\psi_{sc}(kr) \underset{r\to\infty}{\sim} N_l(k)[j_l(kr) - \tan\eta_l^t n_l(kr)], \tag{3.8}$$

where η_l^t is the trial phase shift for the lth potential wave.

3.2 The Kohn functional

The form of the Kohn functional bears a similarity to the Rayleigh-Ritz functional, and is used in a similar fashion, i.e. the stationary solutions are found by solving a set of N linear simultaneous equations. The functional is given by:

$$I = <\Psi^t|L|\Psi^t> = <\Psi^t|2(H-E)|\Psi^t>, \tag{3.9}$$

where H is the total Hamiltonian of the system (reduced to equation (3.4)), and E is the total energy of the system. The exact wave function $R_l(kr)$ is related to Ψ^t by:

$$\Psi^t = R_l(kr) + \delta\phi \tag{3.10}$$

So:

$$\begin{aligned}
\delta I[\Psi^t] &= I[R_l(kr)+\delta\phi] - I[R_l(kr)] \qquad (3.11)\\
&= < R_l(kr)|L|R_l(kr) > + < R_l(kr)|L|\delta\phi > \\
&\quad + < \delta\phi|L|R_l(kr) > + < \delta\phi|L|\delta\phi > \\
&\quad - < R_l(kr)|L|R_l(kr) > \\
&= < R_l(kr)|L|\delta\phi > + < \delta\phi|L|R_l(kr) > \\
&\quad + < \delta\phi|L|\delta\phi > \\
&= < R_l(kr)|L|\delta\phi > - < \delta\phi|L|R_l(kr) > \\
&\quad + < \delta\phi|L|\delta\phi > . \qquad (3.12)
\end{aligned}$$

The second term in equation (3.12) is allowed to be negative because it evaluates to zero. It is neccessary to do this to allow us to use Greens theorem as detailed next. As with the Rayleigh-Ritz method, the last term in equation (3.12) is negligible as it is of second order in the error and can be discarded.

Integrating twice by parts gives us Green's theorem, which states:

$$\int_\tau [f\nabla^2 g - g\nabla^2 f]d\tau = \int_\sigma [f\boldsymbol{\nabla} g - g\boldsymbol{\nabla} f].d\boldsymbol{\sigma} \qquad (3.13)$$

where τ is the volume enclosed by the surface σ. The volume and surface elements are given in polar coordinates by:

$$d\tau = r^2 dr \sin\theta d\theta d\phi \qquad (3.14)$$
$$d\boldsymbol{\sigma} = r^2 \sin\theta d\theta d\phi \hat{\mathbf{r}}. \qquad (3.15)$$

Substituting $< R_l(kr)|L|\delta\phi >$ into Green's theorem as $f\nabla^2 g$ we get:

$$\delta I[\Psi^t] = \int_\sigma [R_l(kr)\boldsymbol{\nabla}(\delta\phi) - (\delta\phi)\boldsymbol{\nabla} R_l(kr)].d\boldsymbol{\sigma}. \qquad (3.16)$$

From the asymptotic form of the wave function, we can use equation (3.13) to obtain an equation for $\delta\phi$:

$$\delta\phi \underset{r_1\to\infty}{\sim} \frac{N_l^2(k)}{2r}k(\tan\eta_l^t - \tan\eta_l)(\cos(kr - \frac{l\pi}{2})), \tag{3.17}$$

And substituting $\delta\phi$ and $R_l(kr)$ into Green's equation, we arrive at the general form of the Kohn functional:

$$\begin{aligned} \delta I[\Psi^t] &= N_l^2(k)k(\tan\eta_l^t - \tan\eta_l) && (3.18)\\ &= \tan\eta_l^t - \tan\eta_l. && (3.19) \end{aligned}$$

The more usual form above is obtained by selecting the normalisation factor $N_l = 1/\sqrt{k}$, so rearranging, we get the *variational* estimate of the phase shift:

$$\begin{aligned} \tan\eta_l^v &= \tan\eta_l^t - \delta I[\Psi^t] && (3.20)\\ &= \tan\eta_l^t - < \Psi^t|L|\Psi^t > . && (3.21) \end{aligned}$$

3.3 The total wave function and short range terms

At long range, the total wave function is a product of the target wave function ϕ_T^t and the scattering wave function ψ_{sc}, together with the relevant spherical harmonic $Y_{l,0}(\theta_1, \phi_1)$. To accurately represent the wave function when the positron is close to the target atom, we use Hylleraas functions to represent the correlations between all the particles in the system. The full trial wave function is thus:

$$\Psi^t = S + \tan\eta^t C + \sum_{i=1}^{N} c_i \phi_i, \tag{3.22}$$

where, using the nomenclature of figure (2.1),

$$S = Y_{l,0}(\theta_1, \phi_1)\sqrt{k} j_l(kr_1)\phi_T^t \tag{3.23}$$

$$C = -Y_{l,0}(\theta_1, \phi_1)\sqrt{k} n_l(kr_1)\phi_T^t, \tag{3.24}$$

and ϕ_i are Hylleraas functions, which for a three-body system are:

$$\phi_i = \exp^{-(\alpha r_1 + \beta r_2 + \gamma r_{12})} r_1^{k_i} r_2^{l_i} r_{12}^{m_i}, \tag{3.25}$$

where k_i, l_i and m_i take non-negative integer values, and are related by the equation:

$$k_i + l_i + m_i \leq \omega. \tag{3.26}$$

The numbers of short-range correlation functions in the wave function, N, generated according to this scheme for ω = 1, 2, 3, 4, 5, 6, 7, 8 are 4, 10, 20, 35, 56, 84, 120, 165 respectively. The normalisation N_l for S and C is merely 1, leaving $\sqrt{k}$ in the terms. Substituting the wave function Ψ^t into (3.21) we have:

$$\begin{aligned} \tan\eta^v &= \tan\eta^t - \sum_{i,j=1}^{N} c_i c_j M_{ij} - 2\sum_{i=1}^{N} c_i Q_i - 2\tan\eta^t \sum_{i=1}^{N} c_i R_i - (S, LS) \\ &\quad -\tan\eta^t (S, LC) - \tan\eta^t (C, LS) - (\tan\eta^t)^2 (C, LC), \end{aligned} \tag{3.27}$$

where $M_{ij} = (\phi_i, L\phi_j)$, $Q_i = (\phi_i, LS)$ and $R_i = (\phi_i, LC)$. As with the Rayleigh-Ritz method, differentiating $\tan\eta^v$ with respect to each of the linear

variational parameters gives a set of (N+1) simultaneous equations which, in matrix form, are:

$$\begin{bmatrix} (C,LC) & \dots & (C,L\phi_j) & \dots \\ \vdots & & \vdots & \\ (\phi_i,LC) & \dots & (\phi_i,L\phi_j) & \dots \\ \vdots & & \vdots & \end{bmatrix} \begin{bmatrix} \tan\eta^t \\ \vdots \\ c_i \\ \vdots \end{bmatrix} = - \begin{bmatrix} (C,LS) \\ \vdots \\ (\phi_i,LS) \\ \vdots \end{bmatrix}, \tag{3.28}$$

where $(C,LS) \equiv < C|L|S >$, and so on. If we express this as

$$\mathbf{AX} = -\mathbf{B} \tag{3.29}$$

then

$$\mathbf{X} = -\mathbf{A^{-1}B} \tag{3.30}$$

and from (3.21) we have:

$$\tan\eta^v = -\begin{bmatrix} \mathbf{X^T} & 1 \end{bmatrix} \begin{bmatrix} \mathbf{A} & \mathbf{B} \\ \mathbf{B^T} & (S,LS) \end{bmatrix} \begin{bmatrix} \mathbf{X} \\ 1 \end{bmatrix} \tag{3.31}$$

$$= -\mathbf{B^T X} - (S,LS). \tag{3.32}$$

The non-linear parameters α, β and γ require optimisation to help convergence of the variational phase shift with respect to an increasing number of linear paramters c_i. This requires that the calculation be repeated for each set of values of α, β and γ.

3.4 Schwartz Singularities

The lower bound for the phase shift usually provided by the Kohn method is not rigorous, the only rigorous lower bound provided is for the scattering length, which translates here to an upper bound on the phase shift, subject to conditions regarding the number of bound states of the potential. This is because, for particular values of α, β and γ, the phase shift may display a *Schwartz* singularity [Sch61]. The number of these singularities increases with the number of short-range terms in the trial function, although the range of values of the non-linear parameters over which they occur will be narrower. The presence of a Schwartz singularity in the Kohn method may be identified by using variants of the Kohn method, as the result generated using the alternative method for the same non-linear parameters may not contain the singularity. The variant used here is the Inverse Kohn method. It uses the same matrix elements as the Kohn method, but involves different matrix manipulations to create the phase shifts.

Chapter 4

Positron-model atom Scattering

The form of the Hamiltonian for the positron-model atom system is, using the nomencalture of figure (2.1), given by:

$$H = -\frac{1}{2}\nabla_1^2 - \frac{1}{2}\nabla_2^2 + V^+(r_1) + V^-(r_2) + V^{\pm}(r_{12}) \tag{4.1}$$

where $V^-(r_2)$ is taken to be the same as in equation (2.1). To complete the model of the system outlined in chapter 2, we introduce the positron-nucleus and the electron-positron potentials:

$$V^+(r_1) = \frac{1}{r_1} + Ae^{-Br_1} \tag{4.2}$$

$$V^{\pm}(r_{12}) = \frac{-1}{r_{12}}. \tag{4.3}$$

The form of $V^+(r_1)$ given here is simply the negative of the attractive electron-nucleus potential, but as we shall see later, this turns out to be too repulsive and so we have also taken $V^+(r_1) = 1/r_1$. Equation (3.22) is the total wave function that H operates on. The energy range to be studied is between the

ground state and the first excited state of the target atom i.e. a positron energy in the range 0 to 23.046 eV (a total energy in the range from -1.1687602 a.u. to -0.32147654 a.u.) Thus, the threshold for excitation lies 0.84728366 a.u. above the ground state.

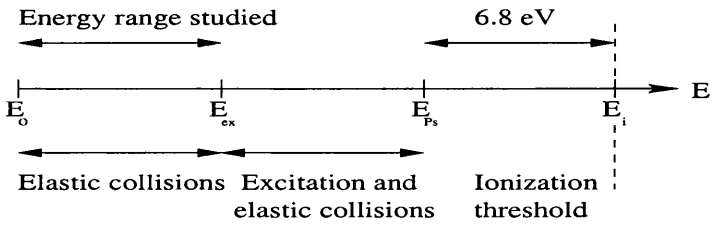

Figure 4.1: Energy spectrum for a positron interacting with the model atom.

A plot of the k dependence of the s-wave phase shift for positron scattering by the model atom is shown in figure (4.1).

The positron-core potential defined by equation (4.2) is so repulsive that the s-wave phase shift becomes progressively more negative as the positron energy increases, but with a slight upturn as the excitation threshold is approached. We have therefore chosen to make the positron-nucleus core potential less repulsive by removing the repulsive exponential term in equation (4.2). This does not affect the model atom, so the results obtained are still useful for indicating the significance of correlations in the model atom. The s-wave phase shift with the new, less repulsive positron-nucleus potential is shown in figure (4.3).

Now the overall positron-atom interaction is sufficiently attractive that the low energy phase shift is positive for low values of k, as it is in positron scattering by atomic hydrogen and helium.

Agreement between the Kohn and inverse Kohn calculations for the phase shift is ususally good, although an identifiable Schwarz singularity is present in the Kohn calculation at $k \simeq 1.00$ a.u.. This is not present in the inverse Kohn calculation.

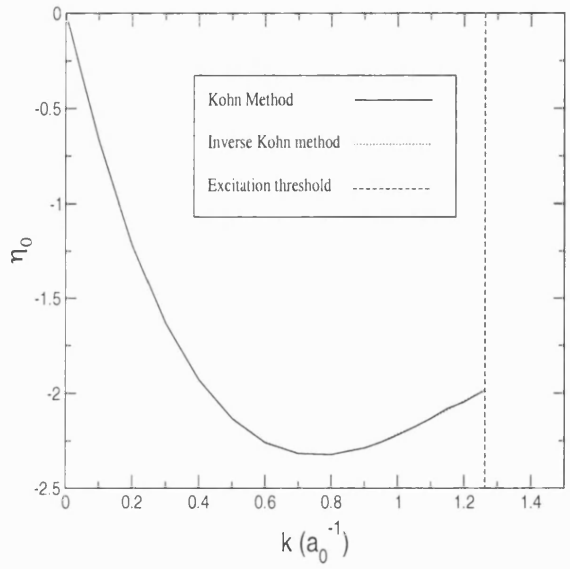

Figure 4.2: Plot of the s-wave phase shift as a function of the positron momentum k, with the original highly repulsive positron-core potential. Note that the agreement between the Kohn and Inverse Kohn methods is so close that the curves overlap.

The phase shifts are well converged with respect to ω, the order of the short range Hylleraas functions. Increasing ω, the sum of the powers of r_1, r_2 and r_3, also increases the number of Hylleraas terms, and hence allows more flexibility in modelling the short range correlations in the system. A good indication of the suitability of the trial wave function is given by the quality of the fit of the data to a convergence plot of the form:

$$\eta(\omega) \;=\; \eta(\omega \;=\; \infty) + \frac{a}{\omega^b}. \tag{4.4}$$

A large value for b indicates a rapid convergence and thus a more suitable wave function.

The degree of convergence of the trial wave function is very good, with $b = 3.56178$, taking the values of ω from 4 to 8. Low values of ω have been

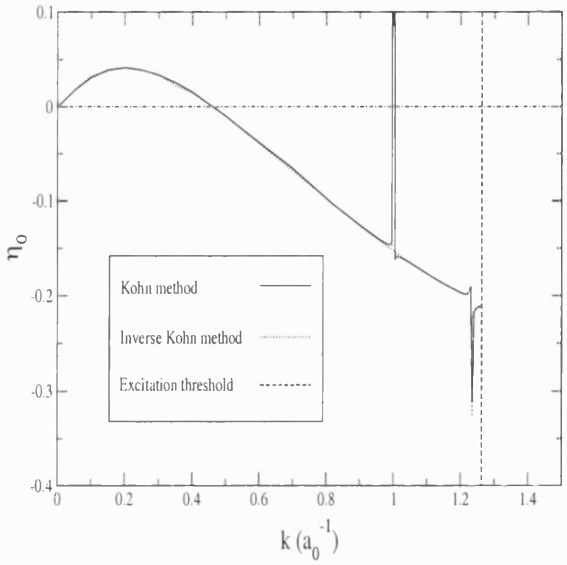

Figure 4.3: Plot of the s-wave phase shift as a function of the positron momentum k with the modified, and less repulsive, $1/r_1$ positron-core potential. A Schwarz singularity is present near to 1.00 a.u., there is also a resonance at k=1.235 a.u..

discarded as the flexibility of the Hylleraas terms is then relatively poor, resulting in a low value for the phase shift when compared to the extrapolated value $\omega(\infty)$ = -0.197146.

Looking at the phase shift again in fig (4.3), we can see the presence of a resonance at k = 1.235 a.u., just below the excitation threshold. At higher energies beyond the resonance, the phase shift increases as expected for the model. The resonance can be attributed to a high degree of correlation between the positron and the atom, and to the presence of virtual excitation.

4.1 The stabilisation technique

One type of resonance that has been clearly found to exist in systems involving positrons are those representing Coulomb bound states in a re-arranged

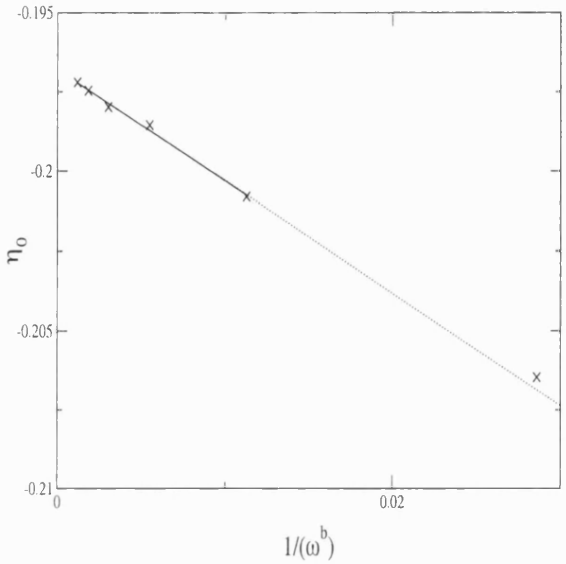

Figure 4.4: Convergence of the s-wave phase shift at $k = 1.2a_0^{-1}$ with respect to increasing ω, with $b = 3.56178$. The results of the inverse Kohn calculation are shown, with the dotted line indicating an extrapolation to other points for lower values of ω not included in the plot.

channel such as for $Ps + H \rightleftharpoons e^+ + H^-$. Other resonances exist such as those occuring just below a threshold for a second reaction channel, known as Feshbach resonances.

To distinguish the type of resonance present we use a technique called the stabilisation method. If there is a resonance, then a good indication of its existence is an *avoided crossing* of two adjacent energy eigenvalues of the matrix representation of the Hamiltonian in the basis of the short range Hylleraas correlation terms in the scattering wave function, so:

$$[< \phi_i|H|\phi_j > -E_n < \phi_i|\phi_j >]\, c_n \;=\; 0 \tag{4.5}$$

which in matrix form is:

$$(\mathbf{H} - E_n\mathbf{S})\mathbf{c} \;=\; 0 \tag{4.6}$$

where

$$\begin{aligned} H_{ij} &= <\phi_i|H|\phi_j>, \\ S_{ij} &= <\phi_i|\phi_j> . \end{aligned} \tag{4.7}$$

i.e. a stabilised or slowly decreasing eigenvalue would have several rapidly decreasing energy levels cutting through it. The presence of a resonance is dependent upon the potential interactions of the whole system, specifically the interaction of the model atom with the positron. A good example of this procedure for finding resonances is shown in figure (4.5). It shows two avoided crossings at an energy of $\simeq -0.4$ a.u., one at $N \approx 41$ and one at $N \approx 100$. This is notably close to the E_1 threshold energy (illustrated) and is indicative of a resonance which is also visible on the plot of the phase shift. This is further evidence that the resonance in the scattering problem is a real feature of the model and not just a numerical anomaly produced by the Kohn method, in a similar fashion to a Schwarz singularity. The variation of the lowest eigenvalue with increasing N also shows that there is no energy of the total system below the energy of the target atom, and therefore no bound state of the positron to the ground state of the target atom. From this lack of a Coulomb bound state, we can conclude that the resonance is a Feshbach resonance, which is present just below the threshold for excitation.

4.2 Virtual excitation

In positron-atom scattering, as the positron is given more energy, the repulsive interactions between the positron and nucleus are overcome, until the positron has enough energy to capture the electron to form positronium (Ps). Below the Ps formation threshold Ps does not possess enough energy to fully separate from the nucleus and so either the Ps dissociates back to produce the positron and the atom, or it annihilates in the vicinity of the nucleus and thus cannot be distinguished from direct positron annihilation.

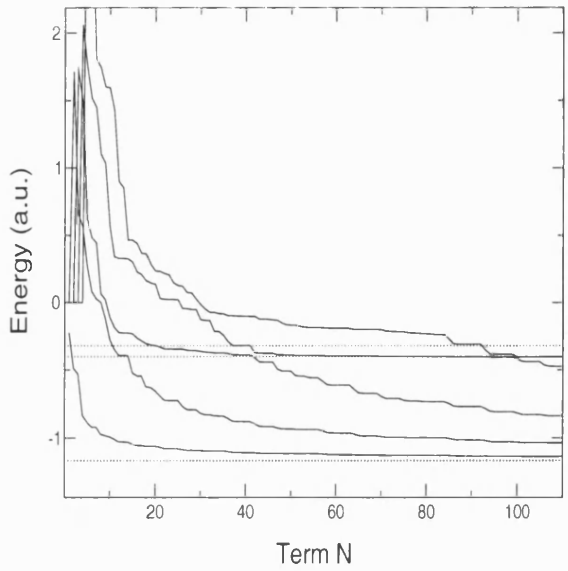

Figure 4.5: The lowest few eigenvalues of the matrix eigenvalue equation (4.5). The lowest dotted line is at the ground state energy of the target atom.

The important point is that through this mechanism of virtual Ps formation, the positron stays in the vicinity of the atom for much longer than usual and hence the rate of annihiliation increases significantly. A similar process is expected to occur just below the excitation threshold, with the positron becoming trapped in the vicinity of the excited atom.

In the model atom presented here, we have introduced a virtual excitation term

$$\frac{e^{-\kappa r_1}}{r_1}(1 - e^{-\lambda r_1})\phi_{ex}(r_2), \tag{4.8}$$

where $\phi_{ex}(r_2)$ is the wave function of the excited target atom and κ is such that

$$\frac{1}{2}k^2 + E_1 = -\frac{1}{2}\kappa^2 + E_2. \tag{4.9}$$

This term represents the excitation of the atom while the positron remains trapped in the vicinity of the model atom.

If this term is included, the phase shift alters significantly. The Hylleraas terms alone do not represent the virtual excitation term very efficiently and so the addition of the virtual excitation term results in significantly more positive phase shifts, as can be seen in figure (4.6). However, if the virtual excitation term, equation (4.6), were not required the Kohn variational method would ensure that its coefficient was small.

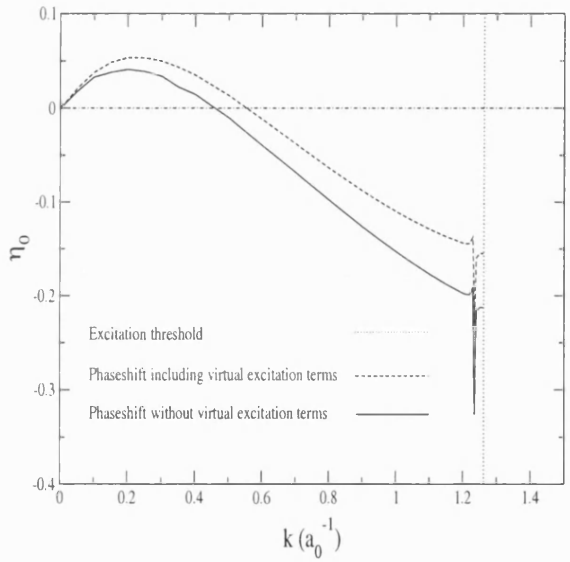

Figure 4.6: Plots of the s-wave phase shift as a function of the positron momentum k with a $1/r_1$ positron-core potential. Only the results for the inverse Kohn method are shown here. The dotted line indicates the position of the excitation threshold.

Convergence of the phase shift with respect to increasing ω is marginally worse with the virtual excitation term included, than without it. This can be explained as a need to re-optimise the non-linear parameters for the wave function to take into account the virtual excitation term.

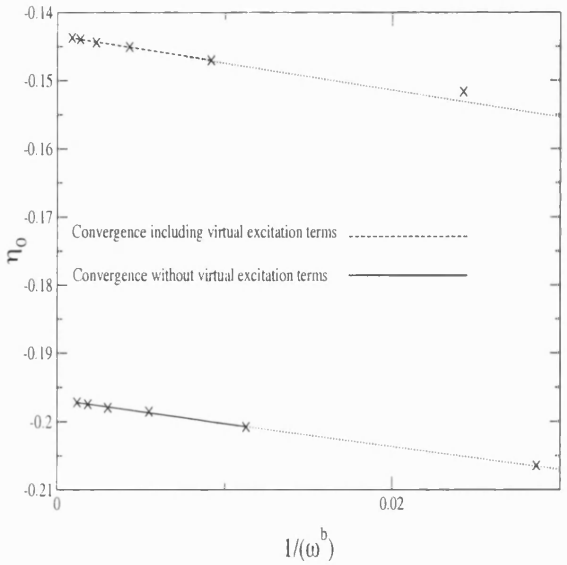

Figure 4.7: Convergence of the s-wave phase shift at $k = 1.2a_0^{-1}$ with respect to increasing ω, for both inclusion and exclusion of the virtual excitation term in the trial wave function ($b = 3.56178$ and 3.32809 respectively). The results of the inverse Kohn calculation are shown, with the dotted line indicating an extrapolation of the line to the results for lower values of ω not included in the plot.

Plots of the s-wave Kohn and inverse Kohn cross sections are presented in figure (4.8), and they both display a resonance-type feature just below the excitation threshold.

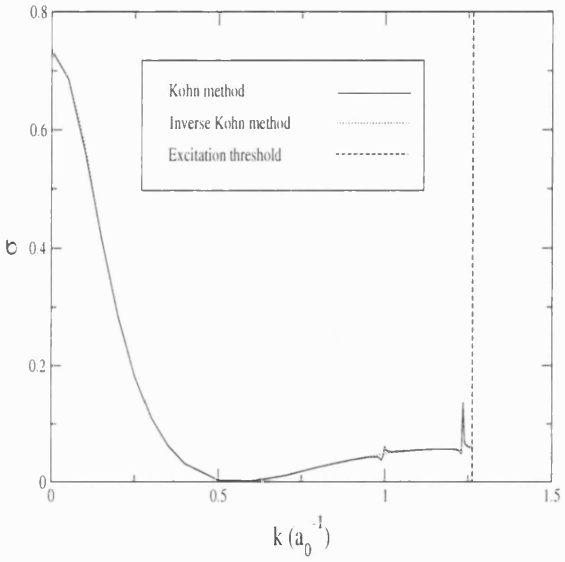

Figure 4.8: The s-wave contribution to the elastic scattering cross section. The feature at $k \simeq 1.0a_0^{-1}$ is only found in the Kohn results and is therefore almost certainly a Schwartz singularity and not a genuine feature of the system.

Chapter 5

Annihilation in Positron-atom Scattering

5.1 Annihilation Rate

Having established the form for the wave function and the phase shifts, we can calculate the annihilation parameter Z_{eff} using the following:

$$Z_{eff} = \sum_{i=2}^{Z+1} \int |\Psi(\boldsymbol{r}_1, \boldsymbol{r}_2, \ldots, \boldsymbol{r}_{Z+1})|^2 \delta(\boldsymbol{r}_1 - \boldsymbol{r}_i) d\boldsymbol{r}_1 d\boldsymbol{r}_2 \ldots d\boldsymbol{r}_{Z+1}. \qquad (5.1)$$

Z_{eff} is a measure of the probability of the positron being at the same position as one of the electrons for the target with Z electrons, each with coordinates $\mathbf{r}_i$ $(i = 2 \ldots, (Z+1))$. Ψ is the scattering wave function for the whole system, normalised to unit positron density asymptotically. The Born approximation yields $Z^B_{eff} = Z$, i.e. $Z^B_{eff} = 1$ for our model atom as there is only one electron in the system. For the present system, the s-wave contribution to Z_{eff} is:

$$Z^0_{eff} = \int |\Psi_0(r_1, r_1 = r_2, r_{12} = 0)| d\boldsymbol{r}_1, \tag{5.2}$$

and the results obtained with the best trial wave function are shown in figure (5.1). The s-wave contribution to the Born approximation to Z_{eff} is also shown there.

The determination of Z_{eff} provides, in some respects, a more rigorous test of the accuracy of the wave function than does the phase shift, as the error in Z_{eff} is only of first order in the error in the wave function, whereas the error in the Kohn phase shift is of second order.

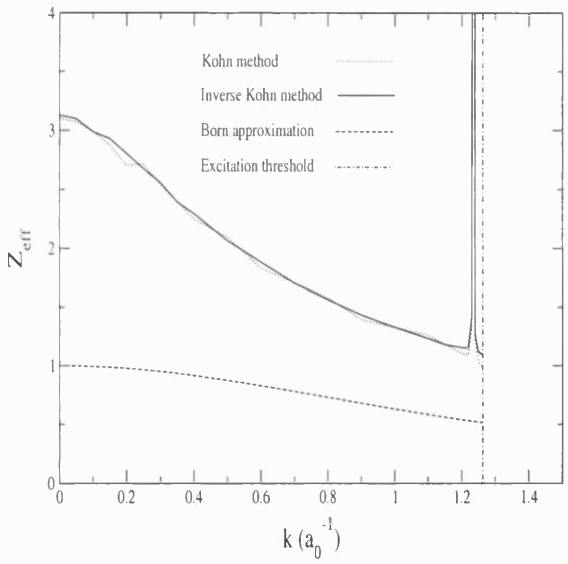

Figure 5.1: The s-wave contribution to Z_{eff} for the model atom system. Virtual excitation terms are included in the trial wave function. Schwartz singularities have been removed for clarity.

It can be clearly seen that the rate of annihilation displays a substantial enhancement close to the excitation threshold. This is both with and without the virtual excitation term, which suggests that the Hylleraas terms can, to

some extent, model the virtual excitation *and* provide a degree of correlation between the atom and the positron.

In a real experiment involving a similar system, the incident positron beam used would have a range of energies, unlike with this theoretical model. Thus, the enhancement in the rate of annihilation close to the excitation threshold would not be as prominent as is found here, as it would be spread out around the feature at 1.23 a.u. to give a broader enhancement curve.

5.2 Angular Correlation

The degree and nature of the positron-target correlation can be explored by examining the total wave function in more detail. Upon annihilation the positron-electron pair can produce either 2 or 3 γ-rays depending on the spin of the system. In the annihilation into 2 γ-rays, the relationships between the momentum of the electron-positron pair and the momentum of the two γ-rays are shown in figure (5.2), for the laboratory frame of reference.

The momenta, $\boldsymbol{p}_1$ and $\boldsymbol{p}_2$, of the Doppler shifted γ-rays are given by

$$\boldsymbol{p}_1 = m\boldsymbol{v} + mc\hat{\boldsymbol{j}} \quad \text{and} \quad \boldsymbol{p}_2 = m\boldsymbol{v} - mc\hat{\boldsymbol{j}}. \tag{5.3}$$

This shift is due to the centre of mass of the positron-electron pair moving with velocity $\boldsymbol{v}$. The magnitude of this Doppler shift is dependent on the velocity of the centre of mass of the electron-positron pair and on the orientation of the emitted γ-rays. At low energies the momentum of each member of the pair is negligible compared to that of each γ-ray, so from figure (5.2) we have

$$p_1 = p_0 + mv\sin\alpha \quad \text{and} \quad p_2 = p_0 - mv\sin\alpha, \tag{5.4}$$

and hence ΔE, the Doppler shift in the energy of each γ-ray, is

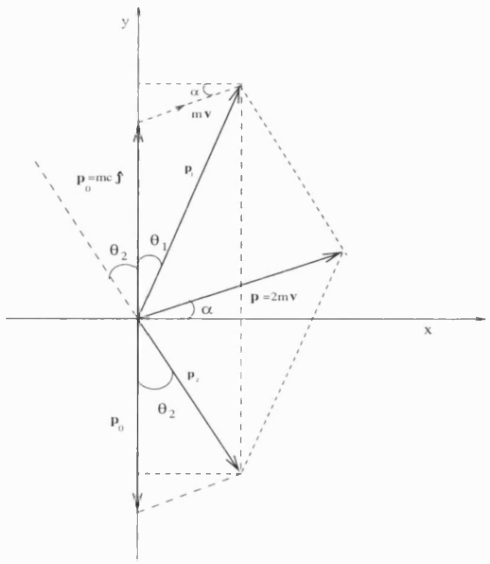

Figure 5.2: Diagram of the momentum relationships between the two γ-rays on annihilation of the positron-electron pair in the laboratory frame of reference.

$$\Delta E = E_1 - E_0 = c(p_1 - mc) = \frac{c}{2}p_y. \tag{5.5}$$

Here E_1 is the energy of the first γ-ray illustrated in figure (5.2), $E_0 = mc^2$ is the energy of each γ-ray in the rest-frame of the annihilating pair, and $\boldsymbol{p} = 2m\boldsymbol{v}$ is the momentum of the pair in the x-y plane in the laboratory frame of reference.

The Doppler-broadened annihilation spectrum is given by the probability distribution function for one of the γ-rays emitted with an energy shift ΔE.

$$F(\Delta E) \propto \int_{-\infty}^{\infty}\int_{-\infty}^{\infty} \Gamma(p_x = \frac{2\Delta E}{c}, p_y, p_z)dp_y dp_z, \tag{5.6}$$

where $\Gamma(\boldsymbol{p})$ is the momentum distribution function. The integral is then evaluated in polar coordinates. $\Gamma(\boldsymbol{p})$ is represented for this positron-model atom system by:

$$F(\boldsymbol{p}) = |\int e^{-i\boldsymbol{p}\cdot\boldsymbol{\rho}}\psi(\boldsymbol{r}_1,\boldsymbol{r}_2)\delta(\boldsymbol{r}_1-\boldsymbol{r}_2)d\boldsymbol{r}_1 d\boldsymbol{r}_2|^2 \quad (5.7)$$

$$= 2\pi|\int_0^\infty \frac{2}{p} sin(pr_1)\psi(r_1)r_1^2 dr_1|^2, \quad (5.8)$$

where $\boldsymbol{\rho} = \frac{1}{2}(\mathbf{r_1}+\mathbf{r_2})$ is the coordinate of the centre of mass of the annihilating positron-electron pair.

As already mentioned, the same information can be obtained from the angle $(\pi - \theta)$ between the two γ-rays:

$$\theta = \theta_1 + \theta_2 = \frac{2mvcos\alpha}{mc} = \frac{p_x}{mc}, \quad (5.9)$$

where p_x is the x-component of the momentum in the x-y plane in the laboratory frame of reference.

Annihilation does not just occur in the x-y plane - it is isotropic, hence we have a relationship between the Doppler shift in energy, ΔE, and the angle θ of the form,

$$\Delta E = mc^2\frac{\theta}{2} = \frac{c}{2}p_x. \quad (5.10)$$

Using this relationship, we can calculate the angular correlation function from the Doppler shift. The angular distribution resulting from this analysis can be compared with that of the undistorted model atom, i.e. using the Born approximation form of the total wave function.

As can be seen in figure (5.3), the undistorted angular correlation function is broader than that of the complete system. A physical explanation of this lies with how tightly bound the electron is in the target. The more tightly bound

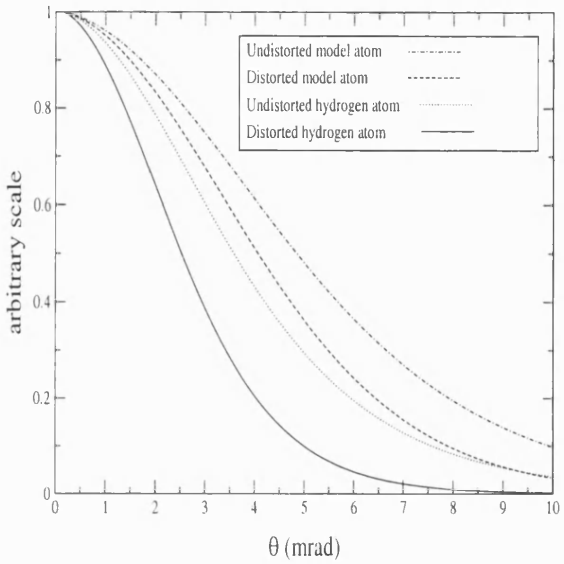

Figure 5.3: Angular correlation function for the two γ-rays produced in the annihilation of a positron with the electron in the target atom.

the electron, the higher its speed will be on annihilation, and therefore the wider the angular distribution. However, the incident positron attracts the electron towards itself and away from the attractive nucleus, thereby reducing the speed of the electron. At the same time, the positron speeds up as it approaches the electron, but the overall effect is to reduce the momentum of the electron-positron pair and therefore to produce a narrower angular correlation curve.

As the model-atom wave function is rather similar to that of hydrogen, it is instructive to compare the angular correlation functions (or Doppler shifts) for the two targets. Unsurprisingly, we see a similarity between the curves for the two targets. However, the model atom has a wider distribution than hydrogen, again due to the binding energy of the electron being larger, and therefore its mean kinetic energy being larger. These distributions have been determined at an incident positron energy very close to zero.

Chapter 6

Summary and Conclusions

The principal purpose of the research reported in this thesis has been to study collisions of positrons with a model atom having the property that its lowest threshold for excitation lay below the threshold for positronium formation, and to investigate whether there might be some enhancement in the positron annihilation rate at incident positron energies close to the excitation threshold. Having first generated a model one-electron atom with the required property, we used the Kohn variational method to determine the elastic scattering phase shift and the total wave function over a range of energies up to the lowest excitation threshold. The resulting wave function was then used to determine the annihilation rate parameter Z_{eff}.

We have shown the presence of a threshold feature in the elastic scattering cross sections close to the excitation threshold for a model atom at an energy corresponding to $k \simeq 1.23$ a.u.. This suggests that there may be similar features at other excitation thresholds in atoms and molecules. The feature is also revealed as a stabilised eigenvalue with a series of avoided crossings at an energy of $\simeq 0.4$ a.u..

We have attributed this feature to a high degree of correlation between the positron and the atom, and to the presence of virtual excited states, which model the temporary formation of a bound state of the positron and the model atom, and its subsequent dissociation back to its original constituents.

We have also found a corresponding increase in the annihilation rate close to the excitation threshold, as the positron becomes temporarily bound to the nucleus for a period of time, thus confirming the significance of the contribution of the virtual excitation terms in the model.

It should be possible, for real experiments using positron beams of increasingly narrow energy resolution, to identify this enhanced annihilation feature close to an excitation boundary for the target in the system, albeit that it is likely to be less prominent (and more broad) than in this model. This is due to the finite energy width of the beam, which along with other reaction channels which may be present in the system, will distort or mask the enhancement.

Further work for this system would involve extending the energy range of the model past the excitation boundary and up to the positronium formation threshold. This would give a more accurate indication of the processes that occur during excitation, and would further confirm the findings presented here. Additionally, from visual representations of the wave function, it may be possible to obtain a better understanding of the correlation changes as the inelastic threshold is approached.

Bibliography

[AAB+] M Amoretti, C Amsler, G Bonomi, A Bouchta, P Bowe, C Carraro, C L Cesar, M Charlton, M J T Collier, M Doser, V Filippini, K S Fine, A Fontana, M C Fujiwara, R Funakoshi, P Genova, J S Hangst, R S Hayano, M H Holzscheiter, L V Jergensen, V Lagomarisino, R Landua, D Lindelöf, E Lodi Rizzini, M Macri, N Madsen, G Manuzio, M Marchesotti, P Montagna, H Pruys, C Regenfus, P Riedler, J Rochet, A Rotondi, G Rouleau, G Testera, A Variola, T L Watson, and D P van der Werf. Production and detection of cold antihydrogen atoms. *Nature*, (419):456.

[BBB+96] G Baur, G Boero, S Brauksiepe, A Buzzo, W Eyrich, R Geyer, D Grzonka, J Hauffe, K Kilian, M LoVetere, M Macri, M Moosburger, R Nellen, W Oelert, S Passagio, A Pozzo, K Röhrich, K Sachs, G Schepers, T Sefzick, R S Simon R, R Stratmann, F Stinzing, and M Wolke. *Phys. Lett.*, B(368):251, 1996.

[BCG+98] G Blanford, D C Christian, K Gollwitzer, M Mandelkern, C T Munger, J Schultz, and G Zioulas. *Phys. Lett.*, B(80):3037, 1998.

[CH01] M Charlton and J Humberston. *Positron Physics.* Cambridge University Press, 2001.

[dGL96] E P da Silva, J S E Germane, and M A P Lima. *Phys. Rev. Lett.*, (77):1028, 1996.

[Dir28] P A M Dirac. *Proc. Roy. Soc.*, A(117):610, 1928.

[Dun02] J T Dunn. *Theoretical Studies of Low Energy Positron-Atom and Atom-Antiatom Collisions.* PhD thesis, UCL, 2002.

[GBO+02] G Gabrielse, N S Bowden, P Oxley, A Speck, C H Storry, J N Tan, M Wessels, D Grzonka, W Oelert, G Schepers, T Sefzick, J Walz, H Pittner, T W Hnsch, and E A Hessels. Background-free observation of cold antihydrogen with field-ionization analysis of its states. *Phys. Rev. Lett.*, (89):213401, 233401, 2002.

[GBSS02] S J Gilbert, L D Barnes, J P Sullivan, and C M Surko. Vibrational-resonance enhancement of positron annihilation in molecules. *Phys. Rev. Lett.*, (88):043201, 2002.

[Gri00] G F Gribakin. *Phys. Rev.*, A(61):022720, 2000.

[HDX+93] L D Hulett Jr., D L Donohue, J Xu, T A Lewis, S A McLuckey, and G L Glish. *Chem. Phys. Lett.*, (216):236, 1993.

[HVWM97] J W Humberston, P Van Reeth, M S T Watts, and W E Meyerhof. Positron-hydrogen scattering in the vicinity of the positronium threshold. *J. Phys.*, B(30):2477, 1997.

[HW72] J W Humberston and J B G Wallace. *J. Phys.*, B(5):1138, 1972.

[IGG+00] K Iwata, G F Gribakin, R G Greaves, C Kurz, and C M Surko. *Phys. Rev.*, A(61):022719, 2000.

[KS90] W E Kauppila and T S Stein. *adv. At. Mol. Phys.*, (26):1079, 1990.

[KSS+81] W E Kauppila, T S Stein, J H Smart, M S Dababneh, Y K Ho, J P Downing, and V Pol. *Phys. Rev.*, A(24):725, 1981.

[LW97] G Laricchia and C Wilkin. *Phys. Rev. Lett.*, (79):2241, 1997.

[Mil81] A P Mills Jr. *Phys. Rev. Lett.*, (46):717, 1981.

[Moh34] S Mohorovičić. *Astron. Nachr.*, (253):93, 1934.

[Ore49] A Ore. *naturvidenskap Rikke*, 1949. No 9 Univ. of. Bergen, Årbok.

[Pea82] G Peach. *Comments At. Mol. Phys.*, (11):101, 1982.

[RL94] R Ramaty and R E Lingenfelter. *High Energy Astrophysics.* World Scientific, 1994. p32.

[RM97] G Ryzhikh and J Mitroy. *Phys. Rev. Lett.*, (79):4124, 1997.

[RMV98] G Ryzhikh, J Mitroy, and K Varga. *J. Phys.*, B(31):3965, 1998.

[Rua45] A E Ruark. *Phys. Rev.*, (68):278, 1945.

[Sch61] C Schwartz. *Phys. Rev.*, (124):1468, 1961.

[SL88] P J Schultz and K G Lynn. *Rev. Mod. Phys.*, (60):701, 1988.

[SPLW88] C M Surko, A Passner, M Leventhal, and F J Wysocki. *Phys. Rev. Lett.*, (61):1831, 1988.

[Van96] P Van Reeth. *Theoretical Studies of Positronium Formation in Low Energy Positron-Helium Collisions.* PhD thesis, UCL, 1996.

[VH98a] P Van Reeth and J W Humberston. *J. Phys.*, B(31):L621, 1998.

[VH98b] P Van Reeth and J W Humberston. *At. Mol. Phys.*, (31):L231, 1998.

[Whe46] J A Wheeler. *Ann. N.Y. Acad. Sci.*, (48):219, 1946.